

# Traversal time for tunneling: Local aspects

Zvi Kotler and Abraham Nitzan

School of Chemistry, Sackler Faculty of Exact Science, Tel Aviv University, Tel Aviv 69978, Israel

(Received 26 August 1987; accepted 17 November 1987)

The relationship between inelastic tunneling processes and the traversal time for tunneling is studied with emphasis on the local aspects of the tunneling time. Viewed in this framework, the local tunneling time is shown to be a dominant factor in determining the inelastic tunneling probability. It is shown that the Buttiker–Landauer semiclassical formalism, when generalized to the case of local interactions and applied to the calculation of inelastic tunneling probabilities, gives results identical to other perturbation theory calculations such as the Bardeen formula. Analytical results derived for square potential barrier are shown to hold also for strongly biased barriers. Application to inelastic tunneling in typical scanning tunneling microscope configuration are discussed.

## I. INTRODUCTION

There has been a considerable amount of discussion on the issue of the duration of the tunneling process. The different conceptual approaches to this question and some of the different results obtained have been briefly reviewed by Buttiker and Landauer (BL)<sup>1–3</sup> (see in particular Ref. 1 for references to earlier work). One common approach<sup>4</sup> invokes the concept of delay time associated with a scattering process

$$\tau_\phi = \tau_{\text{Re}} \equiv \text{Re} \left\{ -i\hbar S^{-1} \frac{dS}{dE} \right\} = \hbar \frac{\partial \Delta\phi}{\partial E}, \quad (1)$$

where  $E$  is the incident energy,  $S$  is the  $S$  matrix, and where  $\Delta\phi$  is the phase shift. Physically this time is related to the motion of the peak of a wave packet through the tunneling region. It has been argued<sup>1,5</sup> that this time, although well defined for all energies, has some intuitively unphysical implications. Instead, in one dimension and in the WKB limit for energies well below the barrier peak, Buttiker and Landauer suggest the time

$$\tau = \int_{x_1}^{x_2} dx [m/\hbar\kappa(x)], \quad (2)$$

where  $x_1$  and  $x_2$  are the turning points of the barrier motion and where

$$\kappa(x) = \frac{1}{\hbar} \{2m[U(x) - E]\}^{1/2} \quad (3)$$

with  $U$  being the potential barrier function, as a measure of the time during which the tunneling particle interacts with the barrier. Pollak and Miller<sup>5,6</sup> have similarly suggested a generalization of Eq. (2),

$$\tau = t_{\text{Im}} \equiv \text{Im} \left( -i\hbar S^{-1} \frac{dS}{dE} \right) = -\frac{1}{2} \hbar |S|^{-2} \frac{d|S|^2}{dE}. \quad (4)$$

The motivations behind Eqs. (2) and (4) are similar. Buttiker and Landauer<sup>1–3</sup> have shown that if a physical process (e.g., energy transfer<sup>1</sup> or Larmor precession<sup>3</sup>) of characteristic time scale  $\omega^{-1}$  occurs within the barrier the inequalities  $\omega\tau \gg 1$  or  $\omega\tau \ll 1$  determine, respectively, the adiabatic or sudden limit with respect to this physical process in much the same way as the real time does for over barrier interactions. Similarly Pollak and Miller<sup>5,6</sup> show that

in the deep tunneling region the magnitude of  $\tau$  determines the extent to which degrees of freedom strongly coupled to the tunneling coordinate have to be quantized.

While the concept of duration of the tunneling process is intellectually appealing, it may be argued that this quantity, being unmeasurable, is of no importance. The significance of the papers discussed above lies in the fact that they point out important consequences of the tunneling time,<sup>7</sup> as implied by the degree of adiabaticity of interactions within the barrier. Two examples of such interactions are: (a) inelastic tunneling<sup>8</sup> and (b) image interactions during tunneling in proximity to metal surfaces.<sup>9</sup> The model advanced in Ref. 8 for inelastic electron tunneling is essentially identical to that used in the discussion of Refs. 1 and 3 of tunneling time. In Ref. 9 the issue of the dynamical image potential felt by an electron tunneling from a metal through a classically forbidden region is discussed with results similar to those of Refs. 1–3.

In the present work we discuss one aspect of the tunneling time not raised by earlier work—its local aspects. Expressions (2) and (4) are associated with the total tunneling process. However, implications related to the degree of adiabaticity of interactions within the barrier are expected to depend also on the range of such interactions and on their location within the barrier. Can we define a time of tunneling between *any* two points  $x_1 < x_2$  within the barrier and associate it with Eq. (2)? We show below that the answer is yes.

Our interest in this problem is motivated by the important potential applicability of scanning tunneling microscopy (STM) to studying adsorbed molecules by inelastic electron tunneling.<sup>10–12</sup> STM by its very nature is extremely sensitive to local aspects of barrier interactions. For the STM configuration with its extremely narrow barrier, it is not clear that perturbative approaches like that of Refs. 1–3 and 8, or the widely used Bardeen's transfer Hamiltonian theory<sup>13</sup> are sufficient. In the next section we take up this issue and compare, for an exactly soluble inelastic tunneling model, calculations based on the perturbative approximations to the exact results. We show that perturbation theories have a wide range of applicability in typical STM configurations, although their limits are explored by some choice of parameters. In Sec. III we discuss, for a rectangular barrier, the

effect of the location and range of the inelastic interaction on the efficiency of the inelastic tunneling processes. This discussion leads to the conclusion that the Buttiker–Landauer traversal time for tunneling, Eq. (2), may indeed be generalized for local interactions. Thus, a transition from the adiabatic to the sudden limit is observed as the range of interaction decreases, making the *tunneling time through the interaction region* shorter. Some implications of this observation are summarized in Sec. IV.

## II. AN EXACTLY SOLVABLE MODEL AND PERTURBATION THEORIES

Our following discussion focuses on the following model: A particle tunnels through a one-dimensional rectangular barrier and interacts during the tunneling process with a two level system. The wave function for this system is represented as a vector  $[\psi_1(x), \psi_2(x)]^T$  and its time evolution is given by the two coupled equations:

$$\frac{\partial \psi_1(x,t)}{\partial t} = -\frac{i}{\hbar} \left[ -\frac{\hbar^2}{2m} \frac{\partial^2}{\partial x^2} + h_1(x) \right] \psi_1 - \frac{i}{\hbar} V(x) \psi_2, \quad (5a)$$

$$\frac{\partial \psi_2(x,t)}{\partial t} = -\frac{i}{\hbar} \left[ -\frac{\hbar^2}{2m} \frac{\partial^2}{\partial x^2} + h_2(x) \right] \psi_2 - \frac{i}{\hbar} V(x) \psi_1, \quad (5b)$$

with

$$h_1(x) = \begin{cases} 0, & |x| > d/2, \\ U, & -d/2 \leq x \leq d/2, \end{cases} \quad (6a)$$

$$h_2(x) = h_1(x) + \Delta E, \quad (6b)$$

$$V(x) = \begin{cases} 0, & x < a, x > b, \\ V, & a \leq x \leq b, \end{cases} \quad (7)$$

$$-\frac{d}{2} \leq a; \quad b \leq \frac{d}{2}. \quad (8)$$

This is a tunneling process involving a particle moving on two parallel potential surfaces (Fig. 1) with position dependent interaction between them. A particle incident on the barrier from the left, moving on surface 1 (i.e., with the two level system in its ground state) may be transmitted or reflected either elastically (on surface 1) or inelastically (on surface 2). Due to the simple geometry the probabilities for these processes may be evaluated exactly by standard methods. The result for the reflection  $r$  and transmission  $t$  amplitudes for the elastic channel and for the corresponding quantities  $\bar{r}$  and  $\bar{t}$  of the inelastic are (see the Appendix)

$$\begin{aligned} r &= \alpha M^{-1}(1,1) + \beta M^{-1}(1,2), \\ t &= \alpha M^{-1}(6,1) + \beta M^{-1}(6,2), \\ \bar{r} &= \alpha M^{-1}(7,1) + \beta M^{-1}(7,2), \\ \bar{t} &= \alpha M^{-1}(12,1) + \beta M^{-1}(12,2), \end{aligned} \quad (9)$$

$|r|^2$ ,  $|\bar{r}|^2$ ,  $|t|^2$ , and  $|\bar{t}|^2$  are the corresponding reflection and transmission coefficients. In particular  $T = |\bar{t}|^2$  corresponds to the inelastic transmission probability. In what follows we shall use a more specific notation, replacing  $t$  by  $t_0$  and  $\bar{t}$  by  $t_+$  or  $t_-$  according to whether the transition occurs from the upper potential surface to the lower one or *vice versa*. The parameters  $\alpha$  and  $\beta$  and the matrix  $M$  are given in the Appendix.

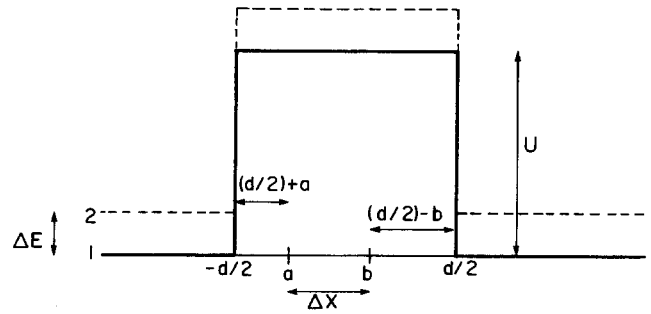


FIG. 1. A two level model for inelastic tunneling through a symmetric square potential barrier. The two potential surfaces are coupled in the region  $a...b$ . The equivalent semiclassical model of Buttiker and Landauer involves one potential surface whose height is modulated in the region  $a...b$ .

A classical analog of this problem is provided by a simple generalization of the model used by Buttiker and Landauer<sup>1,2</sup> (BL). These authors consider tunneling through a rectangular barrier [ $h_1(x)$  say] in the presence of a oscillatory perturbation  $2V(x)\cos(\omega t)$  where  $\omega = \Delta E/\hbar$ .<sup>14</sup> BL take the spatial dependence of  $V(x)$  to be the same as that of the barrier [Eq. (6a)] while we use Eq. (7) in order to be able to discuss the local nature of the tunneling time. The tunneling probability for this model may be solved for  $V \ll \hbar\omega$  using the same perturbation procedure described in Refs. 1 and 2. For the present model this procedure leads to the following expression for the ratio between the inelastic  $t_{\pm}$  and the elastic  $t_0$

$$\frac{t_{\pm}}{t_0} = \frac{2V}{\Delta E} \frac{e^{i(k-k_{\pm})(d/2)}}{B} \times \{\beta(b) - \alpha(b) - [\beta(a) - \alpha(a)]\}, \quad (10)$$

where

$$\alpha(x) = [\kappa_{\pm} \gamma(x) + ik_{\pm} \kappa \eta(x)] \sinh\left[\kappa_{\pm} \left(\frac{d}{2} + x\right)\right], \quad (11a)$$

$$\beta(x) = [\kappa_{\pm} \kappa \eta(x) + ik_{\pm} \kappa_{\pm} \gamma(x)] \times \cosh\left[\kappa_{\pm} \left(\frac{d}{2} + x\right)\right], \quad (11b)$$

$$\gamma(x) = \cosh\left[\kappa \left(\frac{d}{2} - x\right)\right] - i \frac{k}{\kappa} \sinh\left[\kappa \left(\frac{d}{2} - x\right)\right], \quad (11c)$$

$$\eta(x) = \frac{ik}{\kappa} \cosh\left[\kappa \left(\frac{d}{2} - x\right)\right] - \sinh\left[\kappa \left(\frac{d}{2} - x\right)\right], \quad (11d)$$

$$B = 2(k_{\pm}^2 - \kappa_{\pm}^2) \sinh(\kappa_{\pm} d) + 4ik_{\pm} \kappa_{\pm} \cosh(\kappa_{\pm} d), \quad (11e)$$

$$k = \frac{\sqrt{2mE_i}}{\hbar}, \quad \kappa = \frac{\sqrt{2m(U - E_i)}}{\hbar},$$

$$\kappa_{\pm} = \frac{1}{\hbar} \sqrt{2m(U - E_i \mp \Delta E)}, \quad (12)$$

$$k_{\pm} = \frac{1}{\hbar} \sqrt{2m(E_i \pm \Delta E)}.$$

The transmission probabilities  $T_0$  and  $T_{\pm}$  are the absolute squares  $|t_0|^2$  and  $|t_{\pm}|^2$ , respectively.

An alternative perturbation procedure is provided by the Bardeen's transfer Hamiltonian theory<sup>10</sup> which leads to

a golden rule type expression for the transmission rate

$$W_{if} = \frac{2\pi}{\hbar} |\langle \psi_i | H^T | \psi_f \rangle|^2 \rho(E_f), \quad (13)$$

where  $\psi_i$  and  $\psi_f$  are eigenstates of Hamiltonians with semi-infinite barriers. Thus for the problem described by Eqs. (5)–(8) for a particle tunneling from left to right  $\psi_i$  is an eigenfunction of a Hamiltonian with a barrier similar to Eq. (6a) only extended to  $+\infty$  [i.e.,  $h_1(x) = 0$  for  $x < -d/2$  and  $h_1(x) = U$  for  $x > -d/2$ ]. Similarly, for inelastic transmission,  $\psi_f$  corresponds to the barrier  $h_2(x) = \Delta E$  for  $x > d/2$  and  $h_2(x) = U + \Delta E$  for  $x < d/2$ . The tunneling Hamiltonian  $H_T$  is, for the inelastic process, identical to  $V(x)$  of Eq. (7) while for elastic tunneling it has been shown by Bardeen<sup>10</sup> to be given essentially by the flux density operator. The relation between the transmission rate equation (13) and the transmission probability  $T$  is for the present model

$$W_{if} = \frac{\hbar k_f}{Lm} T, \quad (14)$$

where  $L$  is the normalization length. This leads, for the inelastic transmission probability in the Bardeen's formalism, to

$$T_{\pm} = \frac{1}{4} \left( \frac{k_{\pm}}{E_{\pm}} \right)^2 L^2 |\langle \psi_f(E \pm \Delta E) | V(x) | \psi_i(E) \rangle|^2. \quad (15)$$

In order to get Eq. (15) we have set  $E_{\pm} = E \pm \Delta E$  with  $k_{\pm}$  the corresponding free particle wave number and have taken

$$\rho(E_{\pm}) = L/2\pi \left[ \left( \frac{\partial E}{\partial k} \right)^{-1} \right]_{E_{\pm}} = (L/2\pi) M / \hbar^2 k_{\pm}. \quad (16)$$

The subscript (–) corresponds to a particle starting from the lower potential surface 1 ending after transmission on

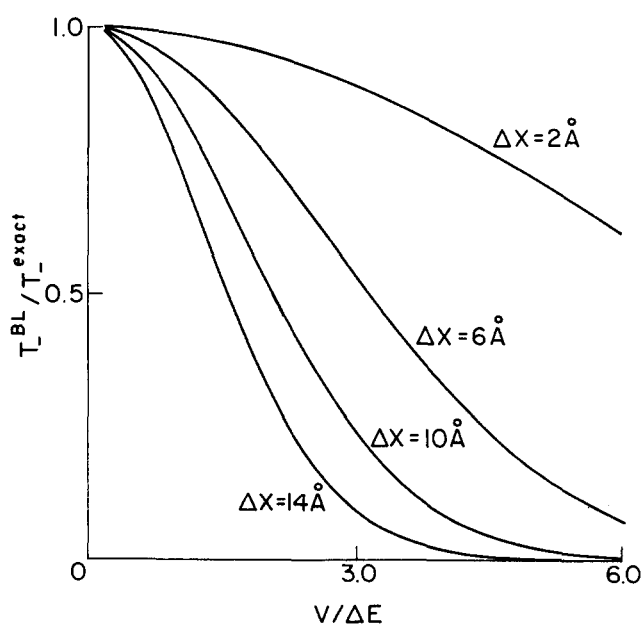


FIG. 2. The ratio  $T_{BL}^{BL}/T_{-}^{exact}$  between the BL result and the exact two level system calculation for  $T_{-}$ .  $U = 10$  eV,  $d = 14$  Å,  $\Delta E = \hbar\omega = 0.5$  eV,  $E_i = 6$  eV. Electron mass is here and in the other figures.

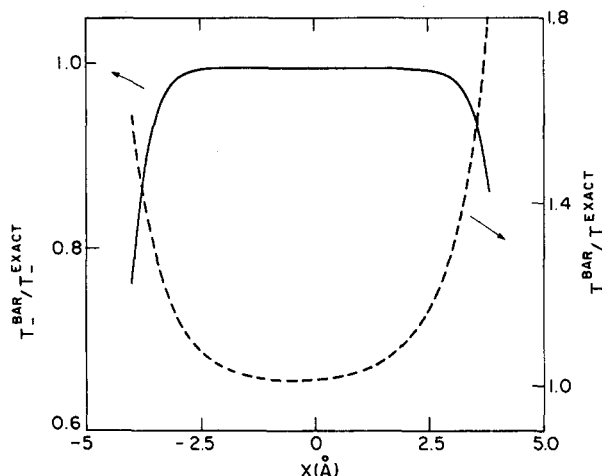


FIG. 3. The ratio  $T_{BAR}^{BAR}/T_{-}^{exact}$  between the result based on the Bardeen approximation and the exact result for a two level system, plotted against the location  $X$  of the excitation region within the barrier. ( $X$  is the center of the excitation region.)  $U = 10$  eV,  $d = 10$  Å,  $\Delta X = 2$  Å,  $\Delta E = 0.5$  eV; full line (left axis)  $E_i = 1$  eV; dashed line (right axis)  $E_i = 9$  eV.

surface 2. The (+) subscript corresponds to the opposite process. Note that in Eq. (15) the normalization length  $L$  cancels out and the result is, of course,  $L$  independent.

Calculations based on Eq. (15) are easier to perform than those based on Eqs. (9) or (10), especially when extensions to nonrectangular situations are carried out. This result is however more restricted than the others because in addition to the requirement  $V \ll \Delta E$  the choice of initial and final wave functions assume that the barrier is thick enough.

In Figs. 2–4 we compare the results for  $T$  from the Buttiker–Landauer (BL) model and of the Bardeen (B) formalism to the exact results obtained from the two level model of Fig. 1. We focus on  $T_{-}$ ; the behavior of  $T_{+}$  being essentially the same. It should be stressed that in the regime where perturbation theory works the results from the Bardeen formalism and those based on the semiclassical BL model are practically identical except when the local interaction is too close to one of the barrier edges. The results in Figs. 2–4 show that the approximate results fail as expected for strong coupling

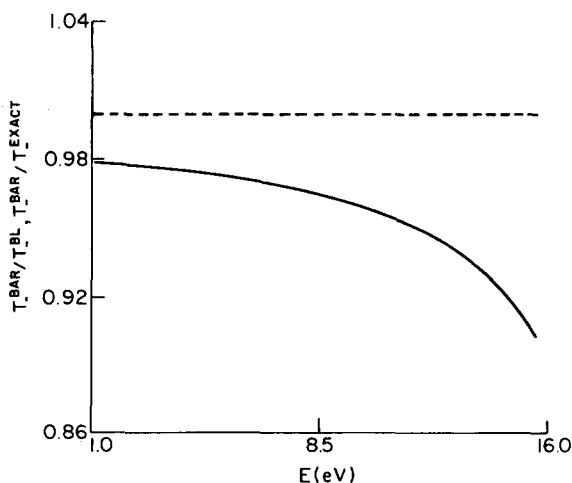


FIG. 4. Full line:  $T_{BAR}^{BAR}/T_{-}^{exact}$ ; dashed line:  $T_{BAR}^{BAR}/T_{BL}^{BL}$  plotted against the incident energy  $E_i$ .  $d = 15$  Å,  $\Delta x = 8$  Å,  $U = 20$  eV,  $\Delta E = 0.5$  eV,  $V = 0.5$  eV.

(a limit which may be reached when  $V/\hbar\omega \gtrsim 1$ , when the interaction region  $\Delta x = b - a$  becomes large, or when the incident energy  $E$  is close to the barrier energy). The result of the Bardeen formalism breaks down also for small  $\Delta x$  when the interaction region approaches one of the edges ( $a \rightarrow -d/2$  or  $b \rightarrow d/2$ ). This behavior is also understandable because near a barrier edge the Bardeen approximation for the wave function describing the particle coming from the other edge fails. This observation is significant for our purpose: The situation where the interaction regime is near the edge of the tunneling barrier is the common one in the STM configuration (molecules adsorbed at an interface).

To end this section we summarize our notation. In what follows we shall use  $t_{\pm}$  and  $T_{\pm} = |t_{\pm}|^2$  for the overall transmission amplitudes and probabilities (respectively) associated with the inelastic components through the barrier.  $t_0$  and  $T_0 = |t_0|^2$  are the corresponding elastic quantities.  $t_{\pm}(d; a, b)$  and the corresponding  $T_{\pm}(d; a, b)$  will denote the inelastic transmission amplitudes and probabilities associated with a barrier of thickness  $d$  [Eq. (6a)] where the inelastic interaction satisfies Eq. (7). In addition we shall denote by  $g_{\pm}(d)$  and  $g_0(d)$  the elastic transmission amplitude through a square barrier of thickness  $d$ , associated with waves of energy  $E \pm \Delta E$  and  $E$ , respectively. Again  $G_{\pm}(d) = |g_{\pm}(d)|^2$  and  $G_0(d) = |g_0(d)|^2$  are the corresponding probabilities. Note that within the perturbative approximation used in the Bardeen's approach, or that used to derive Eq. (10),  $g_0(d) = t_0$ .

### III. LOCAL ASPECTS

In Sec. I we have pointed out, following Buttiker and Landauer,<sup>1-3</sup> the intimate relation between the probability of inelastic tunneling and the adiabaticity of the interaction within the barrier as measured by the tunneling time defined by Eq. (2). When the range of the inelastic interaction is smaller than the barrier width we expect the relevant time to be related to the motion through the interaction regime. In this case however another factor plays an essential role in determining the inelastic current: Consider, for example, the

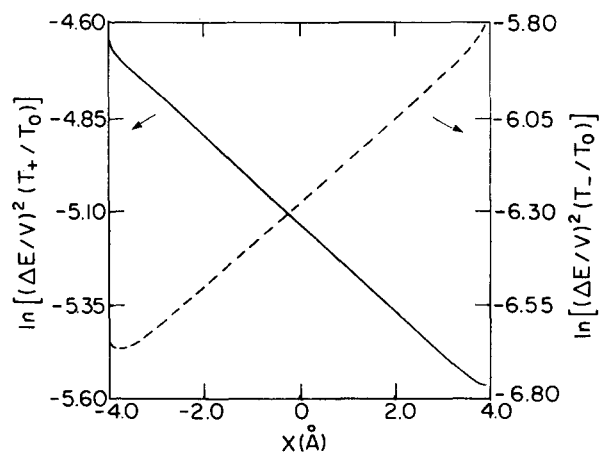


FIG. 5  $T_{\pm}/T_0$  as a function of position of the interaction region. Full line (left axis):  $T_{+}/T_0$ . Dashed line (right axis):  $T_{-}/T_0$ .  $U = 10$  eV,  $E_i = 5$  eV,  $d = 10$  Å,  $\Delta E = 0.5$  eV,  $\Delta V = 0.1$  eV,  $\Delta X = 2$  Å.  $X$  is the center of the interaction region,  $X = (a + b)/2$ .

$E - \hbar\omega$  inelastic component of the wave function. This component is populated in the interaction regime, than has to tunnel through the rest of the barrier ( $b < x < d/2$ ) with the reduced energy. On emerging from the tunneling regime this inelastic component will therefore be smaller (relative to the elastic component) for larger distance  $d/2 - b$ . The opposite is true for the  $E + \hbar\omega$  component. This effect is demonstrated in Fig. 5. It has two important consequences:

(a) In normal inelastic tunneling processes involving the  $E - \hbar\omega$  component associated with vibrational frequencies of adsorbed molecules, the inelastic signal is stronger when the electron current flows towards the interface containing the molecules. On reversal of the current direction this inelastic signal will strongly decrease or entirely disappear.

(b) The opposite holds in cases involving initially excited molecules if the  $E + \hbar\omega$  inelastic component is observed. The following experiment suggests itself: monitoring the tunneling current for fixed junction parameters as a function of exciting light frequency. Resonance behavior is expected and the signal will be stronger when the electron current in the barrier flows away from the edge containing the molecules.

Figures 6–8 demonstrate that the concept of local tunneling time is indeed a valid one. In Fig. 6 the data of Fig. 5 is normalized by dividing each component of the tunneling probability  $T_{\pm}$  by the product of the corresponding elastic tunneling probabilities  $G(d/2 + a)G_{\pm}(d/2 - b)$  for the barrier regions before and after the interaction region. Before the interaction region, in  $-d/2 \cdots a$ , the tunneling probability  $G(d/2 + a)$  corresponding to  $E = E_i$  is used. After it, in the region  $b \cdots d/2$ ,  $G_{\pm}(d/2 - b)$  corresponding to  $E = E_i \pm \Delta E$  is the relevant factor. It is seen that after this normalization the relative tunneling probabilities become insensitive to the location of the interaction regime within the barrier, provided that this regime is not too narrow or not too close to the barrier edge.

It is sensitive however to the local tunneling time. To see this we plot in Fig. 7 the quantities  $\gamma_L$  and  $\tilde{\gamma}_L$  defined by

$$\gamma_L = \frac{T_{+} - T_{-}}{T_{+} + T_{-}}, \quad (17a)$$

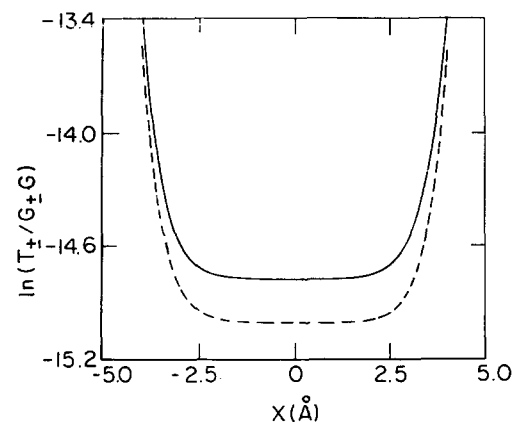


FIG. 6  $T_{\pm}/[G(d/2 + a)G_{\pm}(d/2 - b)]$  as a function of position of the excitation region. Line notations and parameters used are as in Fig. 5.

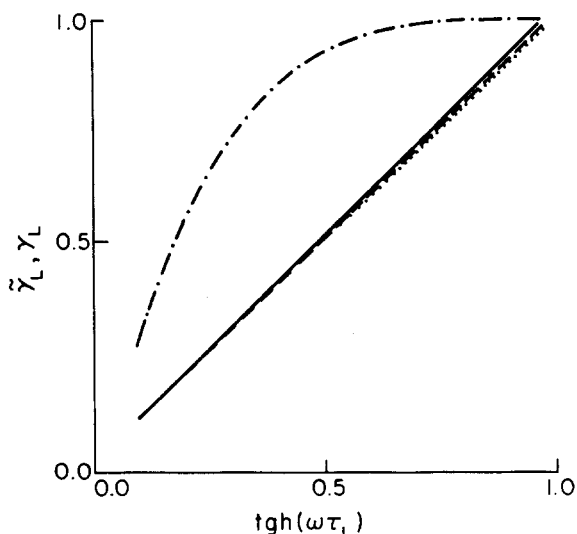


FIG. 7. Full line:  $\gamma = (T_+ - T_-)/(T_+ + T_-)$  as a function of  $\text{tanh}(\omega\tau)$ ;  $\tau = md/\hbar\kappa$ ,  $\kappa = \hbar^{-1} [2m(U - E)]^{1/2}$  for the case where the interaction region exactly overlaps the barrier region.  $U = 10$  eV,  $E_i = 5$  eV,  $d = 30$  Å,  $V = 0.1$  eV, and  $\omega$  is varied. Dashed line:  $\gamma$  as a function of  $\text{tanh}(\omega\tau_L)$ ,  $\tau_L = m\Delta x/(\hbar\kappa)$  for  $\Delta x = 10$  Å with other parameters, the same for the case where the interaction region is at the end of the barrier ( $b = d/2$ ; the incident particle arrives from the other end). Dotted line:  $\tilde{\gamma}_L = (T_+/G_+ - T_-/G_-)/(T_+/G_+ + T_-/G_-)$  as a function of  $\text{tanh}(\omega\tau_L)$  for the case where the interaction regime ( $\Delta x = 10$  Å) is in the middle of the barrier ( $d = 30$  Å).  $G_+$  and  $G_-$  are the elastic transmission probabilities for particles of energy  $E_i + \hbar\omega$  and  $E_i - \hbar\omega$ , respectively, incident on a barrier of thickness 10 Å. Dotted dashed line:  $\gamma$  as a function of  $\text{tanh}(\omega\tau_L)$  for the last case.

$$\tilde{\gamma}_L = \frac{T_+/G_+(d/2 - b) - T_-/G_-(d/2 - b)}{T_+/G_+(d/2 - b) + T_-/G_-(d/2 - b)} \quad (17b)$$

as functions of  $\text{tanh}(\omega\tau_L)$  where  $\tau_L$  is defined by

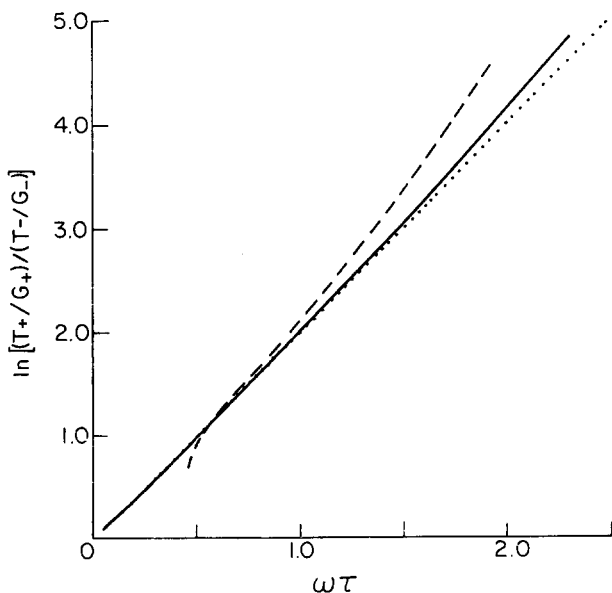


FIG. 8.  $\ln\{[T_+/G_+(d/2 - b)]/[T_-/G_-(d/2 - b)]\}$  plotted against  $\omega\tau$  where the parameter  $\omega\tau$  is controlled in different ways. Full line:  $\omega$  is changed. Dashed line:  $E_i$  is changed,  $\Delta x = 25$  Å,  $U = 20$  eV. Dotted line:  $\Delta x$  is changed ( $E_i = 7.0$  eV). Unless stated otherwise the parameters used are  $d = 50$  Å,  $\Delta x = 10$  Å,  $U = 10$  eV,  $\Delta E = 0.3$  eV,  $V = 0.1$  eV,  $E_i = 5$  eV.

$$\tau_L = \frac{m\Delta x}{\hbar\kappa}, \quad (18)$$

$$\Delta x = b - a; \quad \kappa = \frac{1}{\hbar} [2m(U - E)]^{1/2}. \quad (19)$$

For  $\Delta x = d$  ( $a = -d/2$ ;  $b = d/2$ ), namely the interaction region overlaps exactly the barrier region, the quantities  $\gamma_L$  and  $\tau_L$  are identical to the parameter  $\gamma$  and the tunneling time  $\tau$  defined by Buttiker and Landauer, who have shown that for opaque barriers ( $\kappa d \gg 1$ )  $\gamma = \tanh(\omega\tau)$ .  $\gamma_L$  and  $\tau_L$  are thus the generalizations of  $\gamma$  and  $\tau$  to the local interaction case, and  $\tilde{\gamma}_L$  is the analog of  $\gamma$  in which the differences in the elastic tunneling probabilities in the barrier after the interaction region is normalized out. Figure 7 shows that the expression  $\tilde{\gamma}_L = \tanh(\omega\tau_L)$  is the correct generalization of the BL result.

Figure 8 shows the dependence of the ratio  $T_+/T_-$  on the parameter  $\omega\tau$  where the latter is varied by changing  $\omega$  or by varying  $\tau_L$  ( $\tau_L$  may be controlled by its dependence on  $E_i$  or on the size of the interaction region  $x$ ). It is seen that the transition from the adiabatic ( $\omega\tau \gg 1$ ) to the sudden ( $\omega\tau \ll 1$ ) regime may be achieved by controlling either one of these parameters. In spite of small differences between the three lines it is evident that the local tunneling time is a most important parameter controlling the adiabaticity of the process. It should be kept in mind however that the simple relation between the inelastic tunneling probabilities and  $\tau_L$  breaks down when the barrier is not opaque or even when the interaction range is too narrow (see below).

The results presented in Figs. 5–8 represent either one of the different methods of calculation outlined above. The following analysis is based on the generalized BL expression (10). In the opaque limit where

$$\kappa x, \quad \kappa_{\pm} x \gg 1. \quad (20)$$

for all length parameters

$$x = d, \quad b - a, \quad d/2 - b, \quad d/2 + a \quad (21)$$

we replace  $\sinh(\kappa \pm x)$  and  $\cosh(\kappa \pm x)$  in Eq. (10) by  $\frac{1}{2}e^{\kappa \pm x}$  to get

$$\frac{t_{\pm}(d; a, b)}{t_0} = \frac{V}{2\Delta E} e^{i(k - k_{\pm})d/2} e^{(\kappa - \kappa_{\pm})(d/2 - b)} \times [1 - e^{(\kappa - \kappa_{\pm})(b - a)}] \cdot Z \quad (22)$$

with

$$Z = \frac{(1 + \kappa_{\pm}/\kappa)[(kk_{\pm} - \kappa\kappa_{\pm}) + i(k\kappa_{\pm} + k_{\pm}\kappa)]}{(\kappa_{\pm} - ik_{\pm})^2}. \quad (23)$$

In the opaque barrier limit

$$t_0 \approx g_0(d) = -\frac{4ik\kappa}{(\kappa - ik)^2} e^{-(\kappa + ik)d}, \quad (24)$$

$$g_{\pm}(d) = -\frac{4ik_{\pm}\kappa_{\pm}}{(\kappa_{\pm} - ik_{\pm})^2} e^{-(\kappa_{\pm} + ik_{\pm})d}. \quad (25)$$

We also require the BL result for  $t_{\pm}(b - a; a, b)$ . In the opaque barrier limit this is [cf. Eq. (3.5) of Ref. 2; note that  $V_1$  there corresponds to  $2V$  here]

$$\frac{t_{\pm}(b-a; a, b)}{t_0(b-a)} = -\frac{V}{\hbar\omega} (e^{\pm i\omega\tau_{b-a}} - 1) \exp\left(\mp i \frac{m\omega}{\hbar k} \frac{b-a}{2}\right), \quad (26)$$

$$\tau_{b-a} = \frac{m(b-a)}{\hbar\kappa}. \quad (27)$$

The factors involving  $\omega$  in Eq. (26) arise from the expansions (valid in the opaque barrier limit<sup>1,2</sup>)

$$k_{\pm} = k \pm \frac{m\omega}{\hbar k}, \quad (28)$$

$$\kappa_{\pm} = \kappa \mp \frac{m\omega}{\hbar k}. \quad (29)$$

Therefore Eq. (26) can also be written as

$$\frac{t_{\pm}(b-a; a, b)}{t_0(b-a)} = -\frac{V}{\hbar\omega} (e^{(\kappa-\kappa_{\pm})(b-a)} - 1) e^{i(k-k_{\pm})(b-a)/2}. \quad (30)$$

Equations (22), (24), (25), and (30) may now be combined to give

$$\left| \frac{t_{\pm}(d; a, b)}{t_0(d)} \right|^2 = \left| \frac{t_{\pm}(b-a; a, b)}{g_0(b-a)} \right|^2 \left| \frac{g_{\pm}(d/2-b)}{g_0(d/2-b)} \right|^2 |\bar{Z}|^2, \quad (31)$$

where

$$\bar{Z} = \frac{1}{2} Z \frac{k\kappa(\kappa_{\pm} - ik_{\pm})^2}{k_{\pm} \kappa_{\pm} (\kappa - ik)^2}. \quad (32)$$

If  $k_{\pm} = k$  and  $\kappa_{\pm} = \kappa$ , Eqs. (23) and (32) lead to  $|\bar{Z}|^2 = 1$ . From Eqs. (28) and (29) corrections to this result will be of order  $m\omega/\hbar k^2$  or  $m\omega/\hbar \kappa^2$ . Indeed using Eqs. (23), (28), (29), and (32) we get

$$|\bar{Z}|^2 = 1 \mp \frac{m\omega}{\hbar k^2} \frac{3 - (k/\kappa)^4 + 2(\kappa/k)^2}{(\kappa/k + k/\kappa)^2}. \quad (33)$$

Thus, up to corrections of order  $m\omega/\hbar k^2$ , the product rule anticipated from Figs. 6–9 indeed holds. In particular, the inelastic transition probability is controlled in this limit by the local tunneling time  $\tau_{b-a}$ , Eq. (27), associated with the interaction region. Another interesting observation can be made by using Eqs. (24) to rewrite Eq. (31) in the form

$$|t_{\pm}(d; a, b)|^2 = \left| g_0\left(\frac{d}{2} + a\right) \right|^2 |t_{\pm}(b-a; a, b)|^2 \times \left| g_{\pm}\left(\frac{d}{2} - b\right) \right|^2 \frac{(\kappa^2 + k^2)^2}{16k^2\kappa^2} |\bar{Z}|^2 \quad (34)$$

which shows that within the approximations discussed above the combination  $|t_{\pm}(d; a, b)|^2 / |g(d/2 + a)g_{\pm}(d/2 - b)|^2$  is independent of the location of the interaction region within the barrier (see Fig. 6). More important is the practical computational implication of Eq. (34): It shows that  $t_{\pm}(d; a, b)$  may be calculated as the product of two elastic tunneling probabilities associated with the regions preceding and following the interaction region and

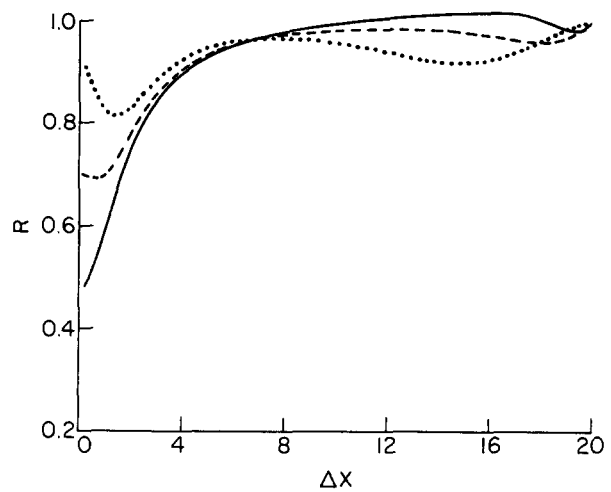
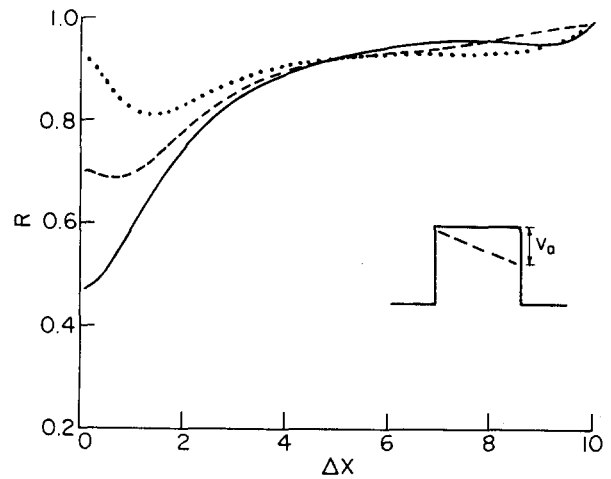


FIG. 9. The ratio  $R$  [Eq. (35)] as a function of  $b-a = \Delta x$ . The excitation region is in the center of the barrier.  $E_i = 3.0$  eV,  $V = 0.1$  eV,  $\Delta E = 0.3$  eV,  $U = 9.0$  eV. In (a)  $d = 10$  Å and (b)  $d = 20$  Å. Full line:  $V_a = 0.0$ ; dashed line:  $V_a = 4.0$  eV; dotted line:  $V_a = 6.0$  eV.

the inelastic tunneling probability associated with the interaction region, times a function of  $k, \omega$ , the incident energy and the barrier height, which does not depend on characteristics of the interaction.

This separation approximation is expected to break down when condition (20) does not hold. This is seen in Fig. 9 where the ratio

$$R = \left| \frac{t_{\pm}(d; a, b)}{g_0(d)} \right| / \left[ \frac{t_{\pm}(b-a; a, b)g_{\pm}(d/2-b)}{g_0(b-a)g_0(d/2-b)} \right] \quad (35)$$

is plotted as a function of  $\Delta x = b-a$ . This ratio should be a constant close to unity when Eq. (31) holds, and the deviation is seen when  $\Delta x$  becomes too small.

In Fig. 9 we have also presented results of calculations of the same ratio defined above for a biased barrier model [see inset to Fig. 9(a)]. The magnitude of the bias is expressed in terms of the energy  $V_a$  defined in the inset. These calculations are based on a numerical study of inelastic tunneling in a two state (Fig. 1) biased barrier model to be described

elsewhere.<sup>17</sup> It is seen that the separation approximation remains valid under the same conditions as discussed above, also in the biased barrier case.

#### IV. CONCLUSIONS

We have shown, for the square barrier and square interaction region model that the provided interaction region is not too narrow and not too close to the barrier edge, the local tunneling time (18) dominates the inelastic tunneling probability. More generally, Eqs. (31) and (34) show that under these conditions the inelastic tunneling probability for the local interaction model can be evaluated in terms of the inelastic tunneling probability for the square barrier associated with the interaction regimes, and elastic tunneling components associated with the other barrier regions. Our calculations for a biased barrier indicate that this result is of more general validity (the concept of local tunneling time was recently considered for a general barrier by Leavens and Aers<sup>18</sup>). Generalizations to higher dimensional potentials may be possible using the formalism of Auerbach and Kivelson.<sup>19</sup>

In addition, we have shown that for standard STM configurations the assumptions inherent in perturbative approaches such as the Bardeen and the Buttiker–Landauer treatments may break down. In particular, the narrow gaps involved in the scanning tunneling spectroscopy configuration requires that the use of the Bardeen formalism should be carried out with caution. When it fails the two level system within a square or biased square potential barrier model can be handled exactly. Otherwise, different methods, possibly direct numerical solution of the Schrödinger equation will have to be used.

#### ACKNOWLEDGMENTS

This research was supported in part by the U.S./Israel Binational Science Foundation and by a PACER Fellowship Grant of Control Data Corporation.

#### APPENDIX

The transmission and reflection coefficients for tunneling in the two level system of Fig. 1 are obtained following the derivation of Puri and Schaich<sup>12</sup>: The wave function in each channel and in any regime I is written as a linear combination  $\Psi_{CI}(x) = \sum_j a_j^{CI} e^{ik_j^{CI}x}$  where the (generally complex)  $k_j^{CI}$ 's are eigenvalues of the coupled problem in regime I. The coefficients  $a_j^{CI}$  are obtained from the continuity equations which are satisfied separately for the wave function of each channel and from the coupled channel equations obtained from the Schrödinger equation. This leads to a set of linear equations of the form

$$\begin{aligned} M(1,1) &= (ik_0 - \kappa_0)e^{(\kappa_0 + ik_0)d/2 + \kappa_0 a}, \\ M(1,2) &= (\kappa_0 + \bar{\kappa}_0)e^{\bar{\kappa}_0 a}, \\ M(1,3) &= (\kappa_0 + \bar{\kappa}_1)e^{\bar{\kappa}_1 a}, \end{aligned}$$

$$M \cdot \begin{pmatrix} r \\ a_1 \\ a_2 \\ a_3 \\ a_4 \\ t \\ \bar{r} \\ \bar{a}_1 \\ \bar{a}_2 \\ \bar{a}_3 \\ \bar{a}_4 \\ \bar{t} \end{pmatrix} = \begin{pmatrix} \alpha \\ \beta \\ 0 \\ 0 \\ 0 \\ 0 \\ 0 \\ 0 \\ 0 \\ 0 \\ 0 \\ 0 \end{pmatrix}, \quad (A1)$$

where

$$\alpha = (\kappa_0 + ik_0)e^{(\kappa_0 - ik_0)d/2} e^{\kappa_0 a}, \quad (A2)$$

$$\beta = (\kappa_0 - ik_0)e^{-(\kappa_0 + ik_0)d/2} e^{\kappa_0 a} \quad (A3)$$

with

$$k_0 = \sqrt{2mE}/\hbar,$$

$$\kappa_0 = \sqrt{2m(U_0 - E)}/\hbar,$$

and  $a$  and  $d$  defined by Fig. 1.  $r$  and  $t$  are the reflection and transmission amplitudes in the elastic channel (so that, e.g.,  $|t|^2$  is the transmission coefficient) and  $\bar{r}$  and  $\bar{t}$  are the corresponding amplitudes in the inelastic channel (the transmittivity being  $|\bar{t}|^2 k_1/k_0$  and reflectivity  $|\bar{r}|^2 k_1/k_0$ ). The coefficients  $a_j$  and  $\bar{a}_j$  ( $j = 1, \dots, 4$ ) define the wave functions in channels 1 and 2 in the interaction zone (a...b) according to

$$\psi_1 = a_1 e^{\bar{\kappa}_0 x} + a_2 e^{\bar{\kappa}_1 x} + a_3 e^{-\bar{\kappa}_0 x} + a_4 e^{-\bar{\kappa}_1 x}, \quad (A4)$$

$$\psi_2 = \bar{a}_1 e^{\bar{\kappa}_1 x} + \bar{a}_2 e^{\bar{\kappa}_0 x} + \bar{a}_3 e^{-\bar{\kappa}_1 x} + \bar{a}_4 e^{-\bar{\kappa}_0 x}, \quad (A5)$$

where

$$\bar{\kappa}_0 = \left( \frac{2m}{\hbar^2} \left[ U_c - E + \frac{\Delta E}{2} [1 - \sqrt{1 + (2V/\Delta E)^2}] \right] \right)^{1/2}, \quad (A6)$$

$$\bar{\kappa}_1 = \left( \frac{2m}{\hbar^2} \left[ U_c - E + \frac{\Delta E}{2} [1 + \sqrt{1 + (2V/\Delta E)^2}] \right] \right)^{1/2}, \quad (A7)$$

$$\kappa_1 = \sqrt{2m(U_0 - E + \Delta E)}/\hbar, \quad (A8)$$

$$k_1 = \sqrt{2m(E - \Delta E)}/\hbar. \quad (A9)$$

In Eqs. (A6) and (A7),  $U_c$  represents the barrier height in the interaction region which may be different from the height  $U_0$  of the rest of the barrier. This difference may arise from the fact that the presence of a molecule in the barrier may give rise to diagonal elements in the interaction Hamiltonian, raising or lowering the potential barrier height. In the latter case, inelastic resonance tunneling may occur for incoming energies  $E$  larger than  $U_c$ . Note, that in Fig. 1 and in the calculations presented we have taken  $U_c = U_0$ .

The matrix elements of  $M$  are given by (only nonzero values are denoted)

$$M(2,1) = (ik_0 - \kappa_0)e^{-(\kappa_0 - ik_0)d/2 - \kappa_0 a},$$

$$M(2,3) = (\kappa_0 - \bar{\kappa}_1)e^{\bar{\kappa}_1 a},$$

$$M(2,4) = (\kappa_0 + \bar{\kappa}_0)e^{-\bar{\kappa}_0 a},$$

$$M(1,5) = (\kappa_0 - \bar{\kappa}_1)e^{-\bar{\kappa}_1 a},$$

$$M(3,2) = (\kappa_0 + \bar{\kappa}_0)e^{\bar{\kappa}_0 b},$$

$$M(3,3) = (\kappa_0 + \bar{\kappa}_1)e^{\bar{\kappa}_1 b},$$

$$M(3,5) = (\kappa_0 - \bar{\kappa}_1)e^{-\bar{\kappa}_1 b},$$

$$M(3,6) = -(ik_0 + \kappa_0)e^{(ik_0 - \kappa_0)d/2 + \kappa_0 b},$$

$$M(2,5) = (\kappa_0 - \bar{\kappa}_1)e^{-\bar{\kappa}_1 a},$$

$$M(4,3) = (\kappa_0 + \bar{\kappa}_1)e^{\bar{\kappa}_1 b},$$

$$M(4,4) = (\kappa_0 + \bar{\kappa}_1)e^{-\bar{\kappa}_0 b},$$

$$M(4,5) = (\kappa_0 + \bar{\kappa}_1)e^{-\bar{\kappa}_1 b},$$

$$M(4,6) = (ik_0 - \bar{\kappa}_0)e^{(ik_0 + \kappa_0)d/2 - \kappa_0 b}.$$

(A10)

The above list establishes the matrix elements of rows 1–4, associated with the elastic channel. The elements of rows 5–8, related to the inelastic channel, can be derived from the above list by using a simple transformation rule that reads

$$M(i+4, j+6) = M(i, j) \quad (\text{A11})$$

and by interchanging  $k_0$  with  $k_1$ ,  $\kappa_0$  with  $\kappa_1$ , and  $\bar{\kappa}_0$  with  $\bar{\kappa}_1$ . The last four rows (9–12) contain eight nonzero elements, expressing relations between the elastic and inelastic wave functions [see Eqs. (A4) and (A5)]:

$$\begin{aligned} M(9,9) &= M(10,8) = M(11,11) = M(12,10) = 1, \\ M(9,2) &= M(11,4) = \gamma(\bar{\kappa}_0), \\ M(10,3) &= M(12,5) = \gamma(\bar{\kappa}_1), \end{aligned} \quad (\text{A12})$$

where

$$\begin{aligned} \gamma(\bar{\kappa}_0) &= -\frac{\Delta E}{2V} (1 - \sqrt{1 + (2V/\Delta E)^2}), \\ \gamma(\bar{\kappa}_1) &= -\frac{\Delta E}{2V} (1 + \sqrt{1 + (2V/\Delta E)^2}). \end{aligned} \quad (\text{A13})$$

<sup>1</sup>M. Buttiker and R. Landauer, Phys. Lett. **49**, 1739 (1982).

<sup>2</sup>M. Buttiker and R. Landauer, Phys. Scr. **32**, 429 (1985).

<sup>3</sup>M. Buttiker, Phys. Rev. B **27**, 6179 (1983).

<sup>4</sup>E. P. Wigner, Phys. Rev. **98**, 145 (1955).

<sup>5</sup>E. Pollak, J. Chem. Phys. **83**, 1112 (1985).

<sup>6</sup>E. Pollak and W. H. Miller, Phys. Rev. Lett. **53**, 115 (1984).

<sup>7</sup>M. Buttiker in Ref. 3 distinguishes between the dwell time, the traversal time, and the reflection time. In the present work the name tunneling time is used for the traversal time of Refs. 1–3. The referee has pointed out to us that the total tunneling time can be actually directly measured by the temperature  $T_a$  for which above-barrier activation starts to dominate the tunneling rate  $\tau \sim \hbar/k_B T_a$ . To the best of our knowledge this interesting identification has been proven only for inverted parabolic potentials and for low damping.

<sup>8</sup>J. R. Kirtley, D. J. Scalapino, and P. K. Hansma, Phys. Rev. B **14**, 3177 (1976).

<sup>9</sup>M. Jonson, Solid State Commun. **33**, 743 (1980).

<sup>10</sup>D. P. E. Smith, M. D. Kirk, and C. F. Quate, J. Chem. Phys. **86**, 6034 (1987).

<sup>11</sup>B. N. J. Persson and J. E. Demuth, Solid State Commun. **57**, 769 (1986).

<sup>12</sup>B. N. J. Persson and A. Baratof (preprint).

<sup>13</sup>J. Bardeen, Phys. Rev. Lett. **6**, 57 (1961).

<sup>14</sup>In Refs. 1 and 2 the perturbation  $V \cos \omega t$  is taken. The factor 2 is added here to make full correspondence between the BL model and Eqs. (5)–(8) (so that coefficients of Fourier components  $e^{i\omega t}$  are the same).

<sup>15</sup>A. Puri and L. Schaich, Phys. Rev. B **28**, 1781 (1983).

<sup>16</sup>P. S. Bagus, C. J. Nelin, W. Muler, M. R. Philpot, and H. Seki, Phys. Rev. Lett. **58**, 559 (1987).

<sup>17</sup>Z. Kotler and A. Nitzan (to be published).

<sup>18</sup>C. R. Leavens and G. C. Aers, 2nd International Conference on Scanning Tunneling Microscopy/Spectroscopy, Oxnard, CA (1987).

<sup>19</sup>A. Auerbach and S. Kivelson, Nucl. Phys. B **257**, 799 (1985).